

---

## Micromechanisms

H. Guckel

*Phil. Trans. R. Soc. Lond. A* 1995 **353**, 355-366

doi: 10.1098/rsta.1995.0105

---

### Email alerting service

Receive free email alerts when new articles cite this article - sign up in the box at the top right-hand corner of the article or click [here](#)

---

To subscribe to *Phil. Trans. R. Soc. Lond. A* go to:

<http://rsta.royalsocietypublishing.org/subscriptions>

---

# Micromechanisms

BY H. GUCKEL

*Wisconsin Center for Applied Microelectronics, Department of Electrical and Computer Engineering, University of Wisconsin–Madison, 1415 Johnson Drive, Madison, WI 53706-1691, USA*

Micromechanics deals with micromechanisms which fall into two broad categories: sensors and actuators. Since sensors measure some property of their environment, internal sensor power dissipation should be minimized and sensor sensitivity must be maximized. In force sensing, power dissipation has been reduced by ten decades in twenty years. Sensitivity has been increased by twelve decades and is now being limited by thermal noise problems. Practical force sensing via mechanically resonant devices, which can be powered by unmodulated light and sensed by optical reflections, has been demonstrated and has major implications on future sensing systems.

Actuators are devices which do work on their environment. The tool to produce microactuators is still a major problem. X-ray-assisted processing with very large structural heights satisfies most of the tool requirements for microactuators. It has been used, along with assembly, to produce magnetic actuators, such as rotational motors, with 120  $\mu\text{m}$  rotors and rotational speeds of up to 150 000 rpm. A generic linear electrostatic actuator with large travel and large output force per unit chip area addresses practical markets for this evolving technology.

## 1. Introduction

Micromechanisms are devices which are fabricated by using micromechanical tools. The structures fall into two broad classes: sensors and actuators.

Sensors extract information from their environment. They should do this without interference. Energy exchanges between the environment and the sensor must therefore be minimized. Stability, especially long-term stability, of the transduction function is essential and becomes a difficult requirement for typical situations where recalibration cannot be implemented. Micromechanical sensors for which the transduction depends, in part, on the mechanical constants for the sensor construction material achieve reasonable stabilities by very carefully selecting the allowed material base. Single-crystal silicon is typically the material of choice. Metals and polymers are avoided because they age.

Actuators are devices which transfer energy to their environment. Typically, this involves energy storage in the actuator and geometric changes or motion during the transfer process. Since energy storage involves the product of energy density  $\rho_E$  and the active actuator volume  $V_A$ , microactuators will be limited in performance. Because the maximum allowed energy densities improve as one changes from electrostatics to magnetics to pneumatics and hydraulics, actuator performance can be optimized. However, there is a penalty. The micromechanical processing tool which

*Phil. Trans. R. Soc. Lond. A* (1995) **353**, 355–366

*Printed in Great Britain*

355

© 1995 The Royal Society

TEX Paper

produces the devices must accommodate the three-dimensionality of coils in magnetics and tubes in hydraulics and pneumatics. At the same time, the tool must be able to produce structures in which the ratio of the active volume to the physical volume of the actuator is as large as possible. These tool issues make the adaptation of integrated circuit processing techniques (basically two-dimensional procedures) difficult if not impossible for microactuator fabrication. This observation is further amplified by material requirements, which extend from metals and alloys to polymers and ceramics. The ageing and recalibration issue is not very severe because actuators are driven externally and can be monitored by precision sensors to form closed-loop microelectromechanical systems (MEMS).

## 2. Advances in microsensors

Many of today's advances in microsensor technology have their origin in the bulk micromachined pressure transducers of the early 1970s, which played a major role in automotive applications. These single-crystal silicon devices used a pill box, which in part consisted of a thin fully supported deflecting plate with a thickness as small as 25  $\mu\text{m}$  and an area of up to 1  $\text{cm}^2$ . Pressure transduction involved the elastic deformation of the plate with strain to resistance conversion via piezoresistive effects for diffused resistors. Typical power dissipation for these devices was  $5 \times 10^{-3}$  W with a force sensitivity near  $10 \times 10^{-3}$  N. The transducers had one fundamental problem: plate thickness control in timed crystallographic etches, which resulted in large rather thick sensing plates for small differential pressure measurements. The cure for this difficulty came from two technological directions: wafer-to-wafer bonding and surface micromachining.

The basic concept in surface micromachined pressure transducers involves a patterned sacrificial layer, such as an oxide post which is supported by the silicon substrate (Guckel & Burns 1984; Sugiyama *et al.* 1986). This post defines the interior of the pill box if it is covered with, say, polycrystalline silicon and if the oxide is next removed by lateral etching. The deflecting portion of the pill box is now formed from a deposited film with thicknesses in the micrometer range and thickness control of  $\pm 1\%$ . The end result for the automotive transducer was a linear size reduction of roughly a factor of 100 with a consequential force sensitivity increase to approximately  $1 \times 10^{-6}$  N. Figure 1 illustrates the concept and implementation.

Surface micromachining improved the force sensitivity of the sensor. However, with piezoresistive sensing, which was used to make the transducer compatible with the older larger version, power dissipation remained in the mW range and power dissipation per chip area increased by a factor of 10 000. This is clearly not desirable. A solution to this problem must deal with the transduction mechanism itself.

Figure 1 illustrates that the pill box is formed by introducing liquid etches, such as HF, through the channels which are defined via a thin oxide and mask defined geometries. The etch is completed when all oxide in figure 1 has been removed. At this point, all exposed surfaces are either single-crystal silicon or polycrystalline silicon and the pill box is accessible to gas ambients. If pill box structures at this stage are heated in an oxygen ambient, all silicon surfaces will oxidize. This oxidation produces a volume expansion since one volume of silicon typically produces two volumes of silicon dioxide. The etch channels will therefore seal before the cavity geometry is compromised and oxygen transport from the ambient to the cavity interior is interrupted. The residual oxygen in the cavity continues to react and can produce

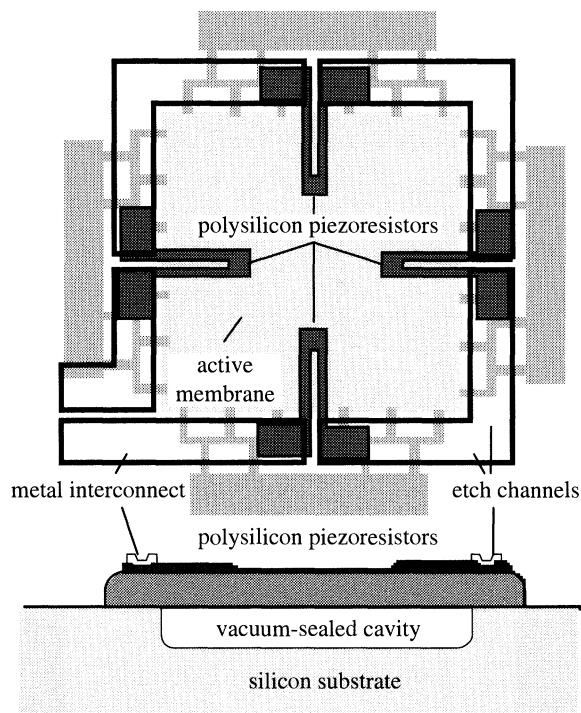


Figure 1. Top and side view of surface micromachined piezoresistive pressure transducer.

a hard vacuum in the sealed pill box. The ability to fabricate pill boxes with hard vacuum by this or similar techniques can be exploited by constructing mechanical resonators with extremely small damping in the cavity interior. This in fact has been done and for clamped-clamped beams the following results have been obtained (Guckel *et al.* 1989).

Polysilicon clamped-clamped beams of 200  $\mu\text{m}$  length, 40  $\mu\text{m}$  width and 2  $\mu\text{m}$  thickness resonate at 500 kHz. The quality factor  $Q$  exceeds 100 000. They measure applied axial loads as the resonant frequency changes. Typical sensitivities are 200 cps  $\text{dyn}^{-1}$ , which implies a force measurement sensitivity of better than  $10^{-10}$  N with standard frequency measurement techniques. Just as important are the driving power requirements. Total energy storage at 100  $\text{\AA}$  deflection is near  $10^{-14}$  J, with a loss of  $10^{-19}$  J per cycle, i.e. roughly 1 eV per cycle, which then leads to an input power of  $10^{-13}$  W. This power is easily supplied via electrostatic excitation, as indicated by figure 2.

The numbers which are quoted here lead to a very different concept in sensor technology. Figure 2 indicates a substrate contact which is fundamentally a pn-junction, which is of course light sensitive. Polysilicon is transparent to photons from the red spectrum, for which both laser and LED sources exist. Since the optical index for silicon is quite high, optical transmission through the outer shell, the upper vacuum gap, the beam and the lower vacuum gap will depend strongly on the geometry of the system. One can take advantage of this by allowing the illumination which reaches the photodiode to be modulated by the beam position. With the correct optical stack design, the open-circuited diode produces a beam-position-dependent voltage which excites the resonance with an unmodulated light beam. This has been achieved in

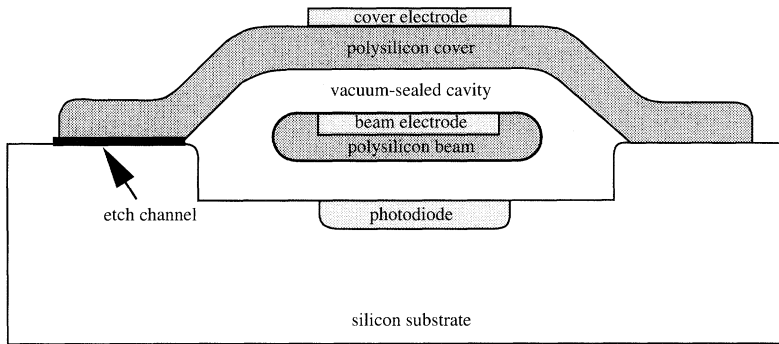


Figure 2. Cross-section of clamped-clamped beam in the vacuum cavity with drive-sense electrode structures.

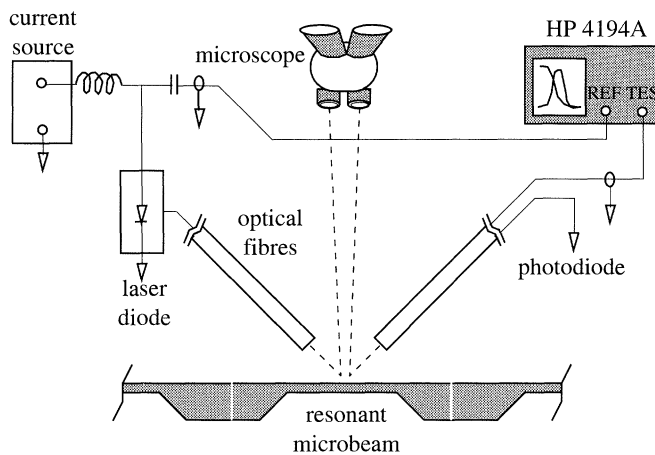


Figure 3. Optical testing of microresonances via unmodulated light excitation.

the laboratory and implies that sensors without wires for either data or power are feasible (Guckel *et al.* 1993*b*).

If one analyses the clamped-clamped beam for the resonator as a spring-mass system, one finds that the system is quite stiff because the spring constant is large. The device is therefore a poor force sensor for static loads which are applied perpendicular to the beam. Force sensing of this type is important in atomic force and tunnelling microscopes where force sensitivity is achieved by small spring constants and optical detection of deflections. Cantilever beams with spring constants in the  $0.01 \text{ N m}^{-1}$  range and detectable displacements of  $1 \text{ \AA}$  produce force sensitivities near  $10^{-12} \text{ N}$  with stored energies of  $10^{-20} \text{ J}$  (MacDonald 1993). This can be improved upon still further by resonating the cantilever system, as for instance in the magnetic resonance force microscope (Rugar *et al.* 1992; Zügar & Rugar 1993). In this type of system, detection limits are set by thermal noise forces which have a white frequency spectrum of the form

$$S_f = 2kT \frac{\hat{k}}{2\pi f_T Q}, \quad (2.1)$$

where  $\hat{k}$  is the spring constant,  $f_T$  is the resonant frequency and  $Q$  is the quality



factor. The minimum detectable force is given by

$$F_{mn} = (S_f \cdot \Delta f)^{1/2}, \quad (2.2)$$

where  $\Delta f$  is the detection bandwidth. This type of system has been shown to have a force sensitivity of  $10^{-15}$  N at room temperature. Low-temperature operation and improved spring design are anticipated to produce force sensitivities of  $10^{-19}$  N.

The discussion may be summarized by noting that commercial quality force sensing has improved from  $10^{-2}$  to  $10^{-12}$  N with a reduction in power dissipation from  $10^{-3}$  to less than  $10^{-13}$  W. These achievements are now just influencing industrial sensing techniques with major implications for optical and magnetic sensing technologies.

In the research area, force sensitivities of  $10^{-15}$  N or 0.1 pg have been achieved at room temperature. A noise-limited sensitivity of  $10^{-19}$  N or 10 ag may be achievable with improved instrumentation at very low temperatures.

### 3. Advances in actuators

Actuators, as stated earlier, are devices which give energy to their environment. Since energy or work involves forces and distances over which the forces act, motion is implied. This observation hints at two major difficulties: three-dimensional construction tools for actuators and limited motion for microactuators.

The construction-tool issue can be clarified by using a wish list approach. Three-dimensionality becomes the first required attribute. This requirement is further complicated by the insistence on tolerances in the 100 ppm range. The third attribute recognizes the fact that actuators are fabricated from many materials: metals and alloys, polymers and ceramics. Since actuators are to become parts of MEMS, the cofabrication of sensors and microelectronic components is required and forms the fourth item on the wish list. Finally, there is the issue of cost effectiveness. This requirement normally leads to the insistence on parallel, rather than serial, manufacturing and favours photoresist-based approaches rather than precision engineering tools. Photoresist-based processing tools typically result in actuator structures with prismatic geometries. For these devices the output force may be written as

$$F = \rho_E V_A, \quad (3.1)$$

where  $\rho_E$  is the energy density which is stored in the active volume of the device. This expression can be written as

$$F/A = \rho_E \alpha H, \quad (3.2)$$

where  $A$  refers to the chip area,  $H$  is the prismatic height and  $\alpha$  is the filling fraction which measures the efficiency with which the processing tool uses the physical volume of the actuator. Since the force per unit area is a figure of merit for actuator construction, processing tools with large achievable structural height are favoured. Furthermore, since  $\alpha$  improves with photoresist resolution, a high-resolution photoresist process with large photoresist thicknesses is very desirable. The LIGA process, which was first discussed by Ehrfeld (Becker *et al.* 1986), meets most of these requirements and is the tool of choice in the current discussion.

The German acronym LIGA stands for lithography, galvo or electroplating and abformung or injection molding. This process is unique in the sense that it recognizes that thick photoresist exposures require large photon energies, to 20 000 eV, which implies X-rays. The required fluxes must also be large because the molecular weight

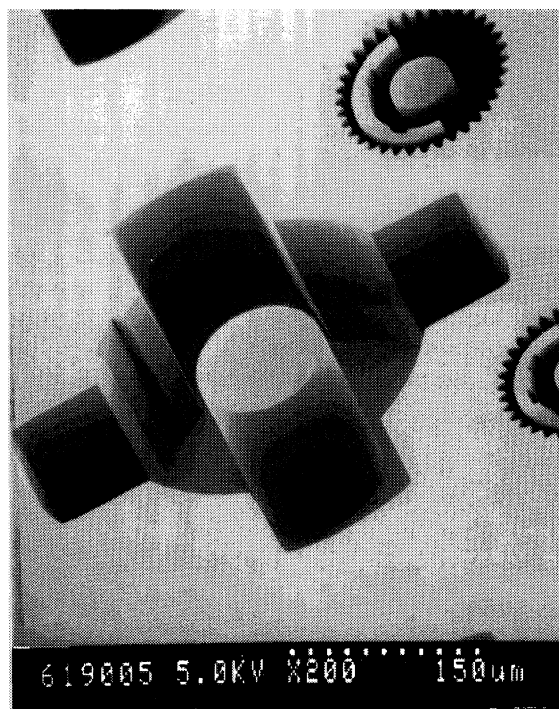


Figure 4. Exposed and developed PMMA. The PMMA thickness is roughly 150  $\mu\text{m}$ .

of large polymer volumes must be modified. Synchrotron radiation from an electron storage ring satisfies both needs and enhances the exposure further by providing photon fluxes which are highly collimated. When this type of exposure source is used in conjunction with an X-ray mask, photo resists such as poly methyl methacrylate (PMMA), expose and develop with essentially vertical flanks. Figure 4 illustrates this point.

The PMMA mold of figure 4 may be converted to a metal mould by applying the photoresist over a plating base and filling the recesses via electro plating. This procedure produces either prototype metal parts or a master metal mold which can be duplicated by injection molding without further use of the synchrotron. This step, injection molding, improves the cost effectiveness of the process.

If one evaluates LIGA against the wish list, one obtains three passes and two fails. The passes originate from cost effectiveness, IC-compatibility and many material issues. The two fails involve the three-dimensionality and tolerance considerations. The tolerance problem is related to the LIGA photoresist application procedure, which is accomplished by casting the polymer in syrup form and subsequent *in situ* polymerization. This procedure involves a 20% volume shrinkage, which causes internal mechanical strain. The built-in strain limits the photoresist height to values below 700  $\mu\text{m}$  and reduces resolution to 5  $\mu\text{m}$  or larger. Both problem areas have been addressed via modified forms of the basic LIGA process (Guckel *et al.* 1991).

LIGA, as demonstrated by figure 4, is a process which produces excellent vertical pattern fidelity. Width variations are less than 0.1  $\mu\text{m}$  per 100  $\mu\text{m}$  of structural height. This property of LIGA may be exploited by producing metal parts which rigidly adhere to the substrate and parts which are free. The free parts may then be

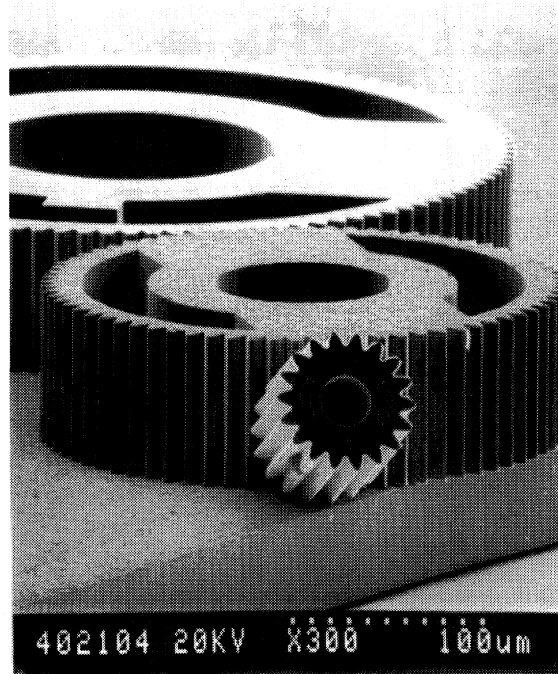


Figure 5. Freed nickel parts of 100  $\mu\text{m}$  height.

assembled with the fixed parts. This procedure enhances three-dimensionality. It also solves the tolerance issue because assembly, in effect, subtracts two large dimensions from each other. The difference between the two dimensions can be in the submicron range.

In order to implement assembly, LIGA can be combined with surface micromachining. In this type of processing a sacrificial layer is applied to the substrate, patterned and covered with the plating base. The LIGA process is then executed and then unwanted plating base segments are removed. The process continues with lateral etching of the sacrificial layer, which produces free or partially attached metal parts. Figure 5 demonstrates the results.

The effectiveness of assembly is demonstrated in figure 6. The difference between shaft diameter and rotor bushing is 0.5  $\mu\text{m}$ , which produces a clearance of 0.25  $\mu\text{m}$  for a height of 100  $\mu\text{m}$ .

Surface micromachining (SLIGA) and LIGA, has evidently solved the tolerance issue. The three-dimensionality has been improved as demonstrated in figure 7.

Further improvements are possible if the photoresist application procedure is modified to avoid the built-in mechanical strain in the PMMA. This has been accomplished by developing a photoresist application procedure, which starts with precast sheets of high molecular weight PMMA (Guckel 1993). The material is essentially strain free because the material is allowed to polymerize without mechanical constraints and is heat treated to remove residual stresses. The material is cut to size by mechanical means and can either be exposed directly or can be solvent bonded to a substrate which is furnished with the plating base. The direct exposure of the PMMA leads to plastic parts such as the gear in figure 8.

The result which figure 8 demonstrates implies that large parts with submicron



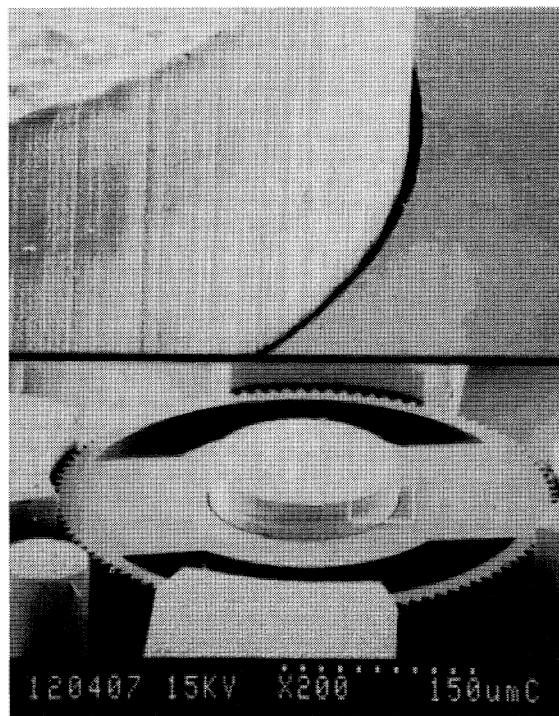


Figure 6. The assembled shaft-rotor combination exhibits submicron clearances.

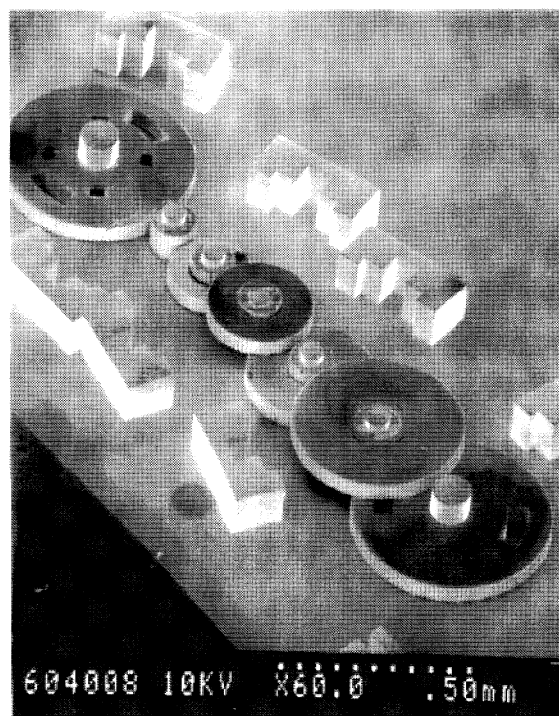


Figure 7. Assembled 60:1 gear box.

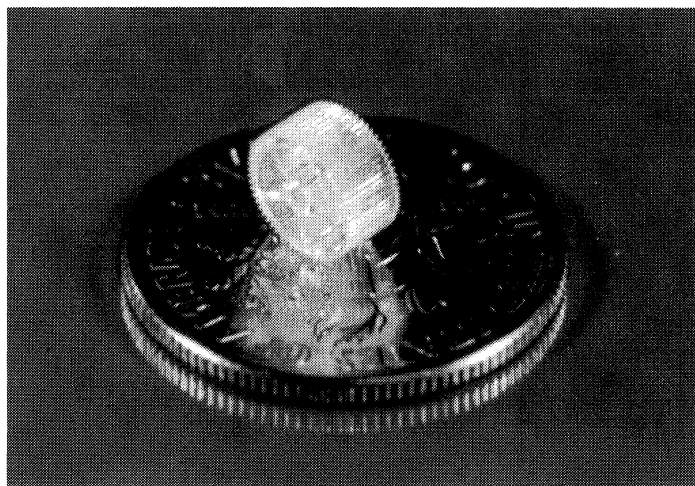


Figure 8. 3 mm thick PMMA gear fabricated from free-standing PMMA sheet on top a dime.

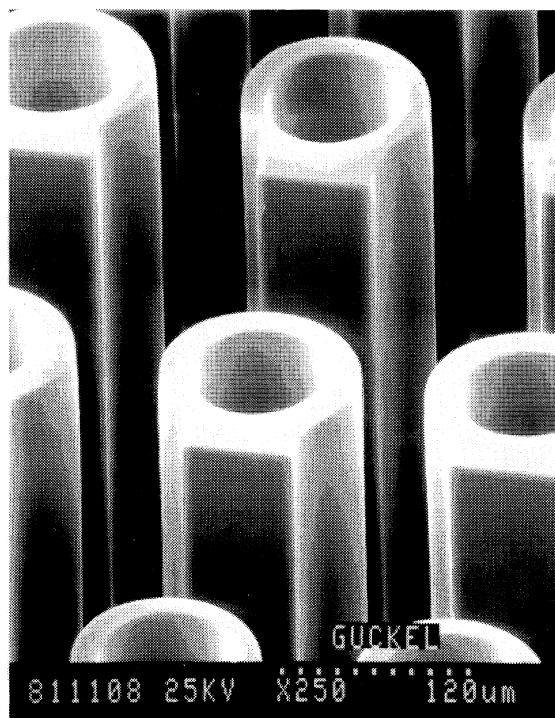


Figure 9. Exposed and developed PMMA pattern with structural height of 3200  $\mu\text{m}$ .

tolerances can be produced with micromechanical tools and that, therefore, precision engineering and micromechanics are related.

If the PMMA sheet is solvent bonded to a substrate, typical LIGA exposures can be attempted. They profit from 20 000 eV photons for which the absorption length in PMMA is 1 cm. Figure 9 illustrates the results.

The strain-free nature of the photoresist process has an additional benefit. It en-



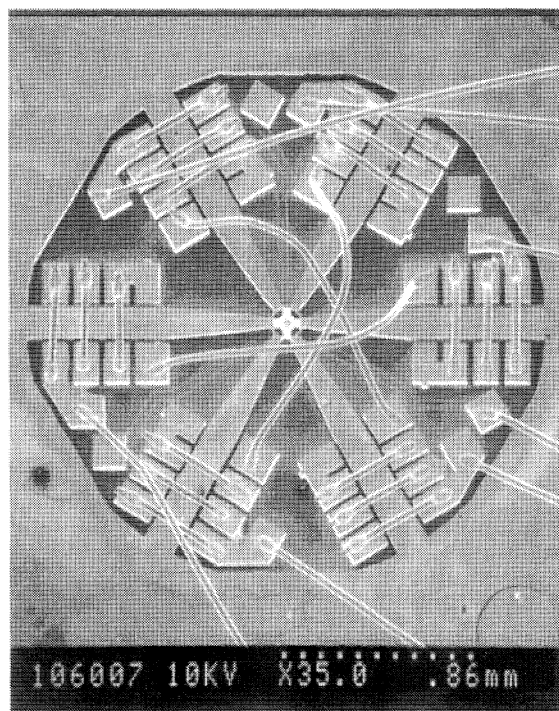


Figure 10. Three-phase micromotor.

ables the use of multiple X-ray masks, which enhances the three-dimensionality still further. Work along these lines is currently in progress and will be combined with future extensions to provide a processing tool which meets all the required attributes of the wish list.

Microactuators fall into two broad categories: rotational machines and linear motors. Either type may use electric or magnetic fields to provide electronically controllable motion. Magnetic actuation produces slightly higher energy densities. However, its main advantage comes from impedance levels which are low, and therefore noise immune, and for which high-speed electronics are readily available. These observations, and the fact that many ferromagnetic materials can be electroplated, favour magnetic actuators. Soft magnetic material, permalloy with 78% nickel and 22% iron, has been plated in LIGA-like procedures and produces as plated an as coercivities of less than 1 Oersted with permeabilities above 2000 and maximum flux densities of 10 000 G (Guckel *et al.* 1993*a*). Hard magnetic materials, typically cobalt alloys, can also be plated and will become available in the future.

The rotational machine which is shown in figure 10 illustrates a fully integrated micromotor.

This mechanism is a three-phase magnetic motor which has been constructed from permalloy. The excitation coils are made in three sections. The lower cross-under is formed from patterned nickel, which is covered with deposited silicon dioxide for dielectric isolation. The vertical sections of the coils are electroplated permalloy. The coil is completed by wire bonding with 25  $\mu\text{m}$  diameter wires. The rotor diameter is 120  $\mu\text{m}$ . Its thickness is less than the stator thickness. This allows the rotor to rise above the substrate surface when the poles are energized. The support shaft is

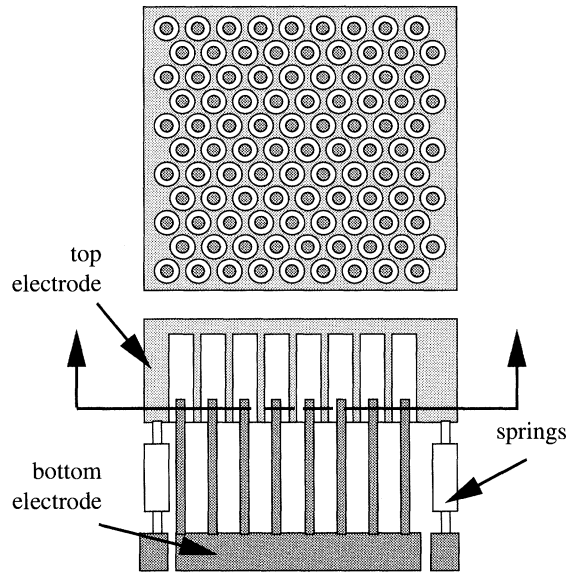


Figure 11. Linear electrostatic actuator design based on LIGA-like processing.

fluted to produce an air-bearing effect, which centres the rotor and thereby minimizes friction. Motor dynamics are monitored by photodiodes which are fabricated in the substrate and act as a primitive shaft encoder.

Open-loop operation in room ambient results in maximum speeds of 150 000 rpm without long-term wear. Speed limits are caused by loss of synchronism due to stepping motor oscillations. These oscillations are related to the low inertia of the rotor and a torque versus rotation angle characteristic with large ripple. Better motor designs and closed loop operation can prevent these difficulties and will produce material-limited speeds above 1 000 000 rpm for gyro-like instruments and perhaps isotope separators.

Linear micromotors typically suffer from low output forces with limited throws. However, these devices have large market potential in such diverse fields as magnetic recording, microrelays, optical multiplexers and positioning systems. Attempts to use LIGA-like processing for this type of actuator are now in progress and are illustrated in figure 11.

The actuator is basically a multi-finger capacitor. The number of fingers per unit area can be very large, which implies a large filling fraction. The finger length and the spring design control the available throw, which in turn is related to the achievable photoresist height and plating depth. Predicted output force is  $1 \text{ N cm}^{-2}$  with maximum throws of 1 cm. Motion control to a few Å is possible.

#### 4. Summary

Good sensors are devices which consume no power and measure some physical property of their environment with large sensitivity. Progress in force sensing over the last 20 years has reduced power requirements from  $10^{-3}$  to  $10^{-13}$  W and increased force sensitivity from  $10^{-2}$  to  $10^{-15}$  N. Further increases in sensitivity are possible but are limited by thermal noise considerations.

The situation for microactuators is quite different. These devices, which do work

on their environment, are difficult to fabricate and suffer from the lack of an adequate processing tool. X-ray-assisted high-aspect-ratio processing fills some of the needs of the tool and has been used to fabricate a variety of actuators with record-setting performances. The use of micromechanical techniques to produce larger devices with submicron tolerances has major implications on traditional precision engineering techniques.

## References

- Becker, E. W., Ehrfeld, W., Hagmann, P., Maner, A. & Münchmeyer, D. 1986 Fabrication of microstructures with high aspect ratios and great structural heights by synchrotron radiation lithography, galvanofarming and plastic moulding (LIGA process). *Microelectron. Engng* **4**, 35–56.
- Guckel, H. 1993 Micromechanics via X-ray assisted processing. Invited talk/paper at *American Vacuum Society 40th National Symp. (Orlando, FL, 15-17/11/1993)*; 1995 *J. Vac. Sci. Technol.* (to be published).
- Guckel, H. & Burns, D. W. 1984 Planar processed polysilicon sealed cavities for pressure transducer arrays. *IEEE-IEDM Technical Digest*, pp. 233. Los Alamitos, CA: IEEE Computer Society Press.
- Guckel, H., Sniogowski, J. J. & Christenson, T. R. 1989 Construction and performance characteristics of polysilicon resonating beam force transducers. In *Proc. 3rd Toyota Conf. (Nissin, Japan, 23/10/1999)* pp. 23-1.
- Guckel, H., Skrobis, K., Christenson, T. R., Klein, J., Han, S., Choi, B. & Lovell, E. G. 1991 Fabrication of assembled micromechanical components via deep X-ray lithography. In *Proc. of IEEE Micro Electro Mechanical Systems (Nara, Japan, 1/1991)* pp. 74–79.
- Guckel, H., Nesnidal, M., Zook, J. D. & Burns, D. W. 1993a Optical drive/sense for high  $Q$  resonant microbeams. In *Transducers '93 Conf. (Yokohama, Japan, 7-10/6/1993)* pp. 686–689.
- Guckel, H., Christenson, T. R., Skrobis, K. J., Klein, J. & Karnowsky, M. 1993b Design and testing of planar magnetic micromotor fabricated by deep X-ray lithography and electroplating. In *Transducers '93 Conf. (Yokohama, Japan, 7-10/6/1993)* pp. 76–79.
- MacDonald, N. C. 1993 Nanomechanisms and tips for microinstruments. In *Proc. 7th Int. Conf. on Sensors and Actuators (Yokohama, Japan, 6/1993)* pp. 8–11.
- Rugar, D., Yannoni, C. S. & Sidles, J. A. 1992 Mechanical detection of magnetic resonance. *Nature* **360**, 563–566.
- Sugiyama, S., Suzuki, T., Kawahama, K., Shimaoka, K., Takigawa, M. & Igarashi, I. 1986 Microdiaphragm pressure sensor. *IEEE-IEDM Technical Digest*, pp. 184–187. Los Alamitos, CA: IEEE Computer Society Press.
- Züger, O. & Rugar, D. 1993 First images from a magnetic resonance force microscope. *Appl. Phys. Lett.* **63**, 2496–2498.



Downloaded from [rsta.royalsocietypublishing.org](http://rsta.royalsocietypublishing.org)

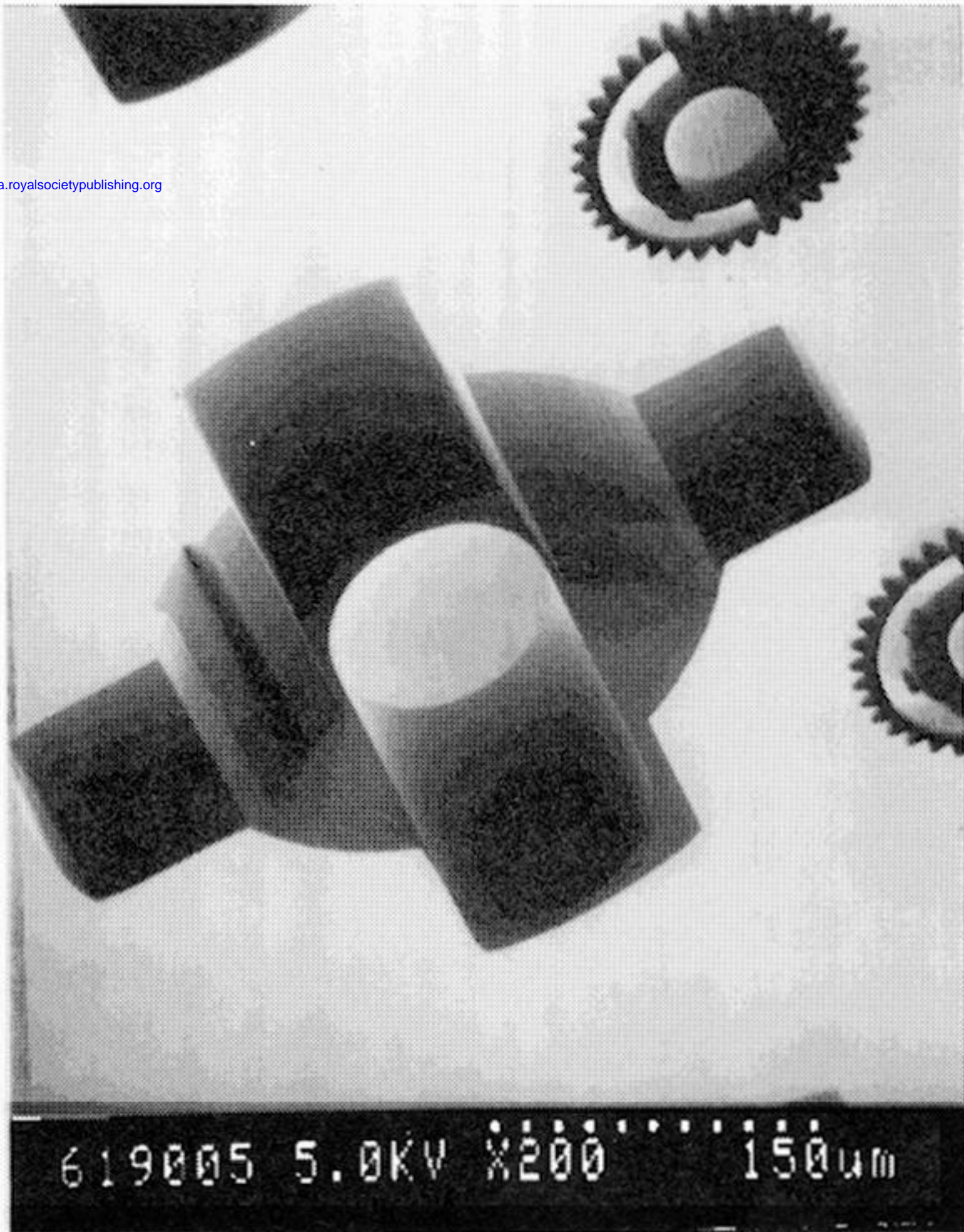


Figure 4. Exposed and developed PMMA. The PMMA thickness is roughly  $150 \mu\text{m}$ .



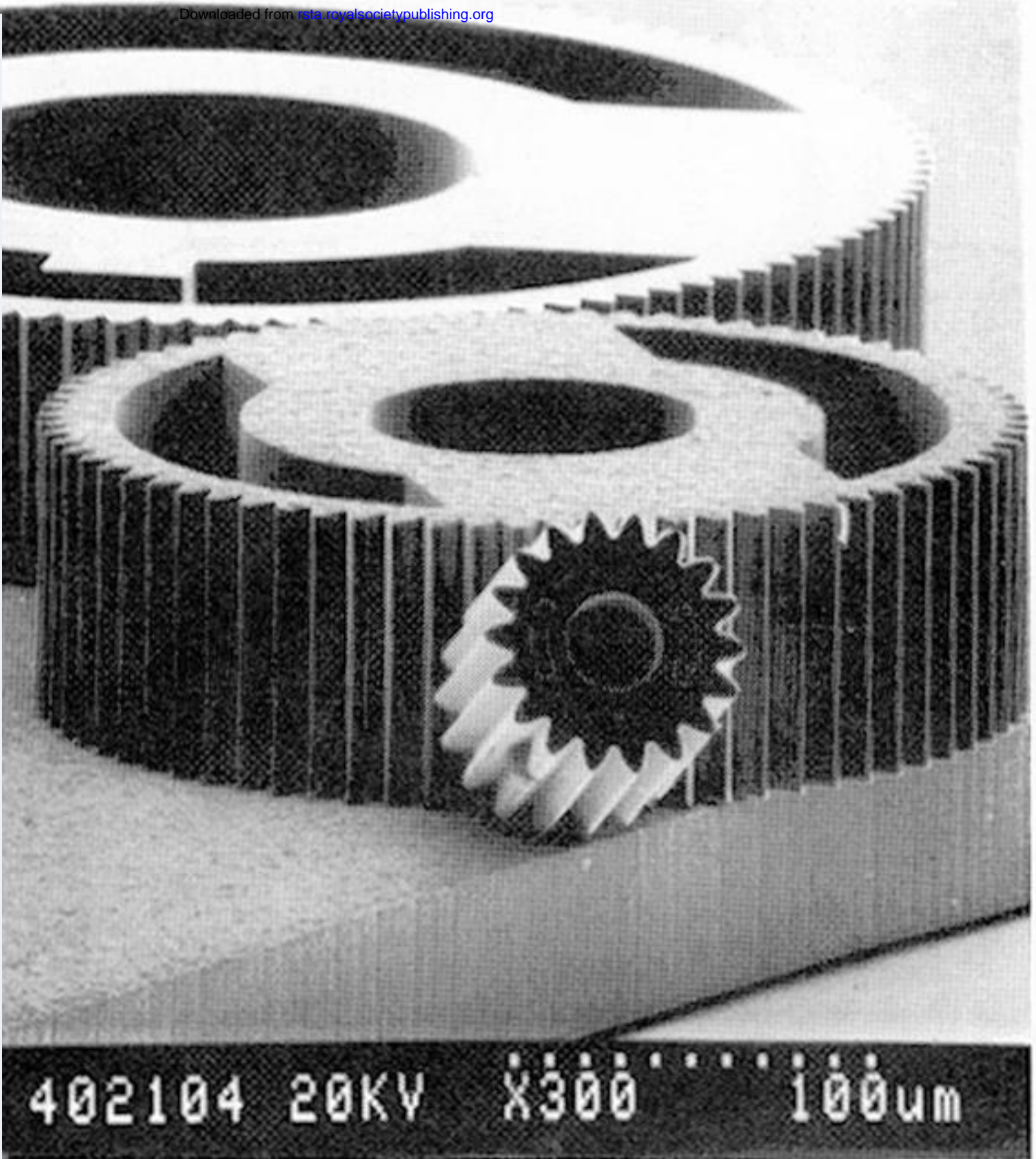


Figure 5. Freed nickel parts of 100  $\mu\text{m}$  height.



Downloaded from [rsta.royalsocietypublishing.org](http://rsta.royalsocietypublishing.org)

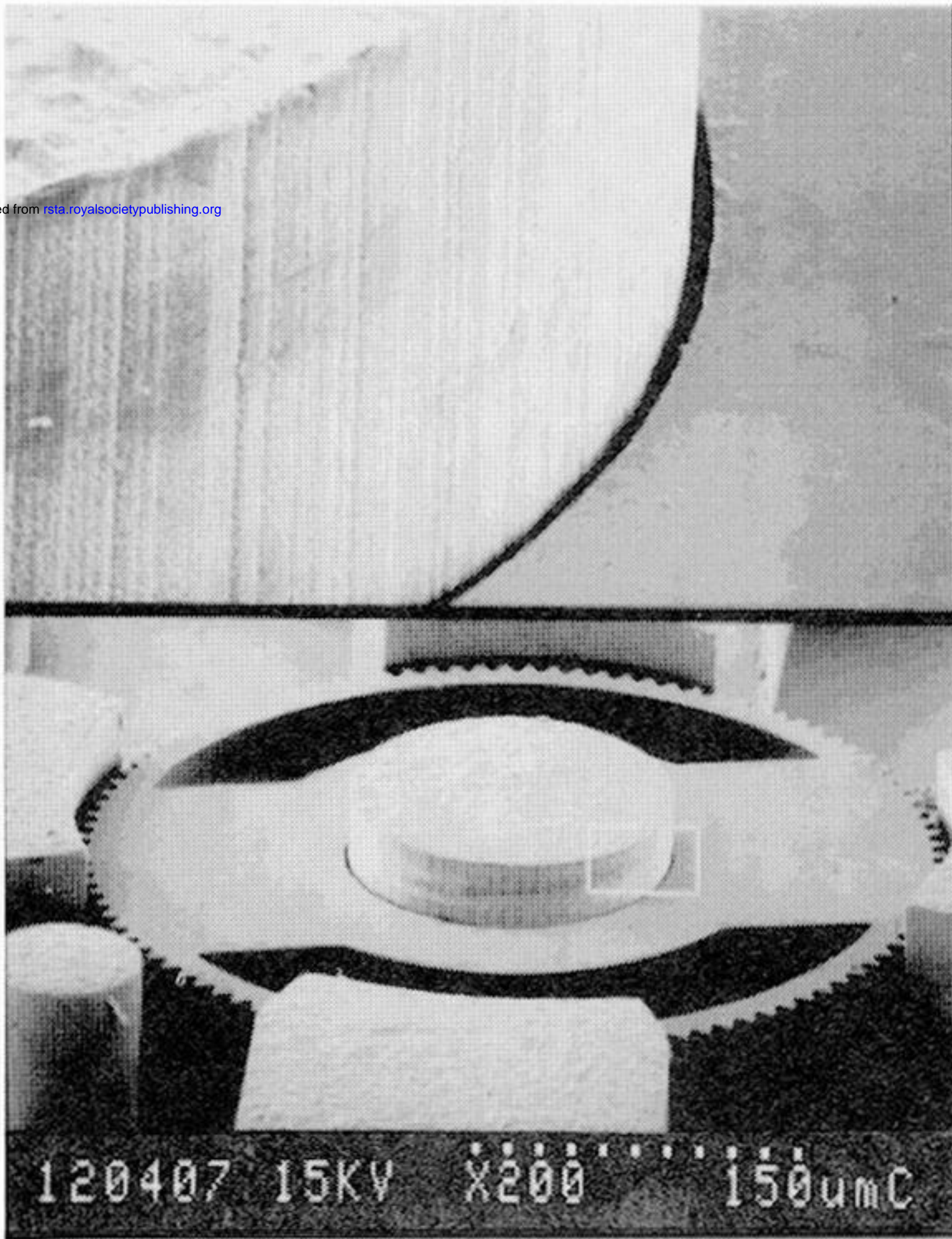


figure 6. The assembled shaft-rotor combination exhibits submicron clearances.



Downloaded from [rsta.royalsocietypublishing.org](http://rsta.royalsocietypublishing.org)

MATHEMATICAL,  
PHYSICAL  
& ENGINEERING  
SCIENCES

THE ROYAL  
SOCIETY

PHILOSOPHICAL  
TRANSACTIONS  
OF

MATHEMATICAL,  
PHYSICAL  
& ENGINEERING  
SCIENCES

THE ROYAL  
SOCIETY

PHILOSOPHICAL  
TRANSACTIONS  
OF

604008 10KV X60.0 .50mm

Figure 7. Assembled 60:1 gear box.



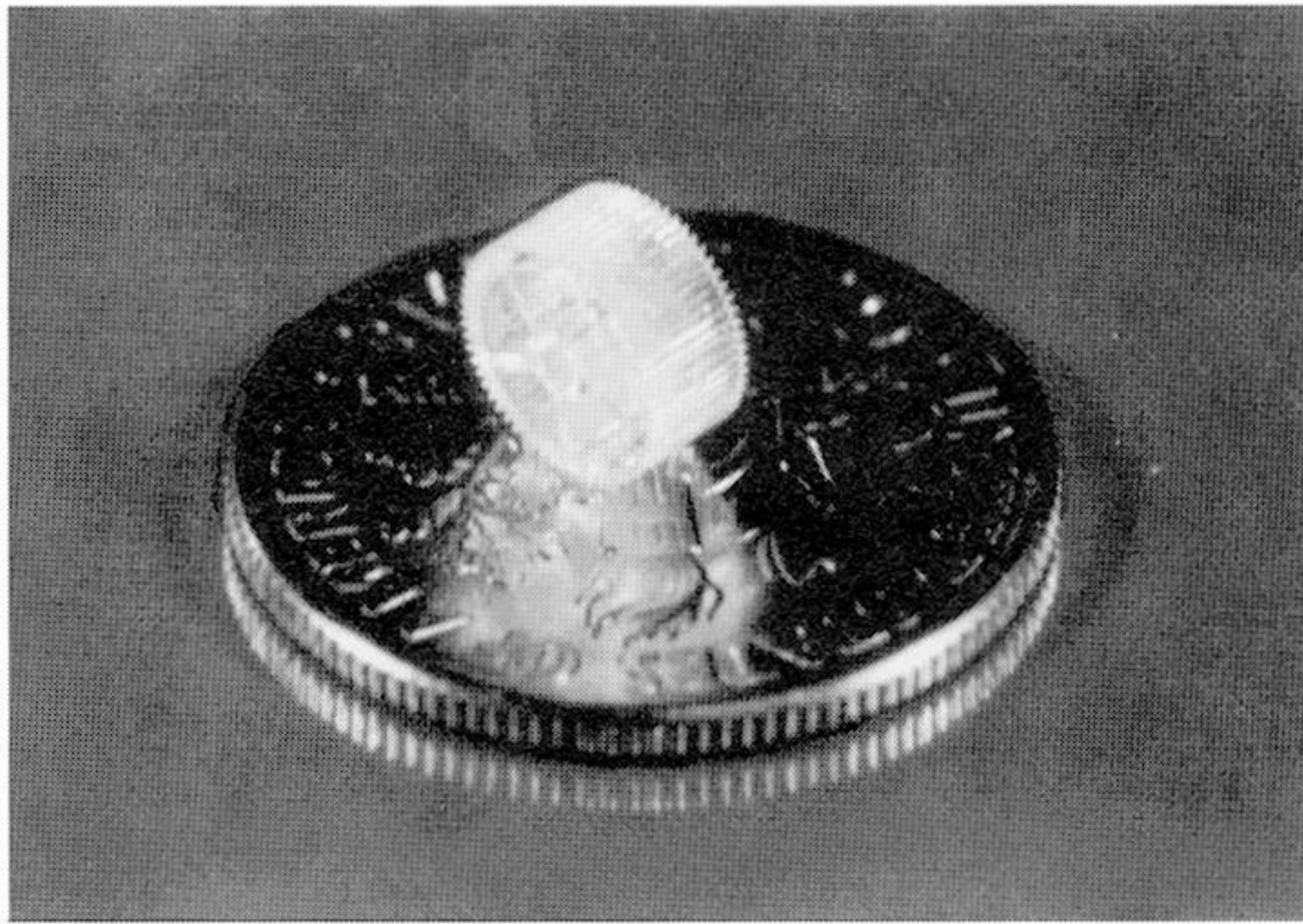


Figure 8. 3 mm thick PMMA gear fabricated from free-standing PMMA sheet on top a dime.



Downloaded from [rsta.royalsocietypublishing.org](http://rsta.royalsocietypublishing.org)

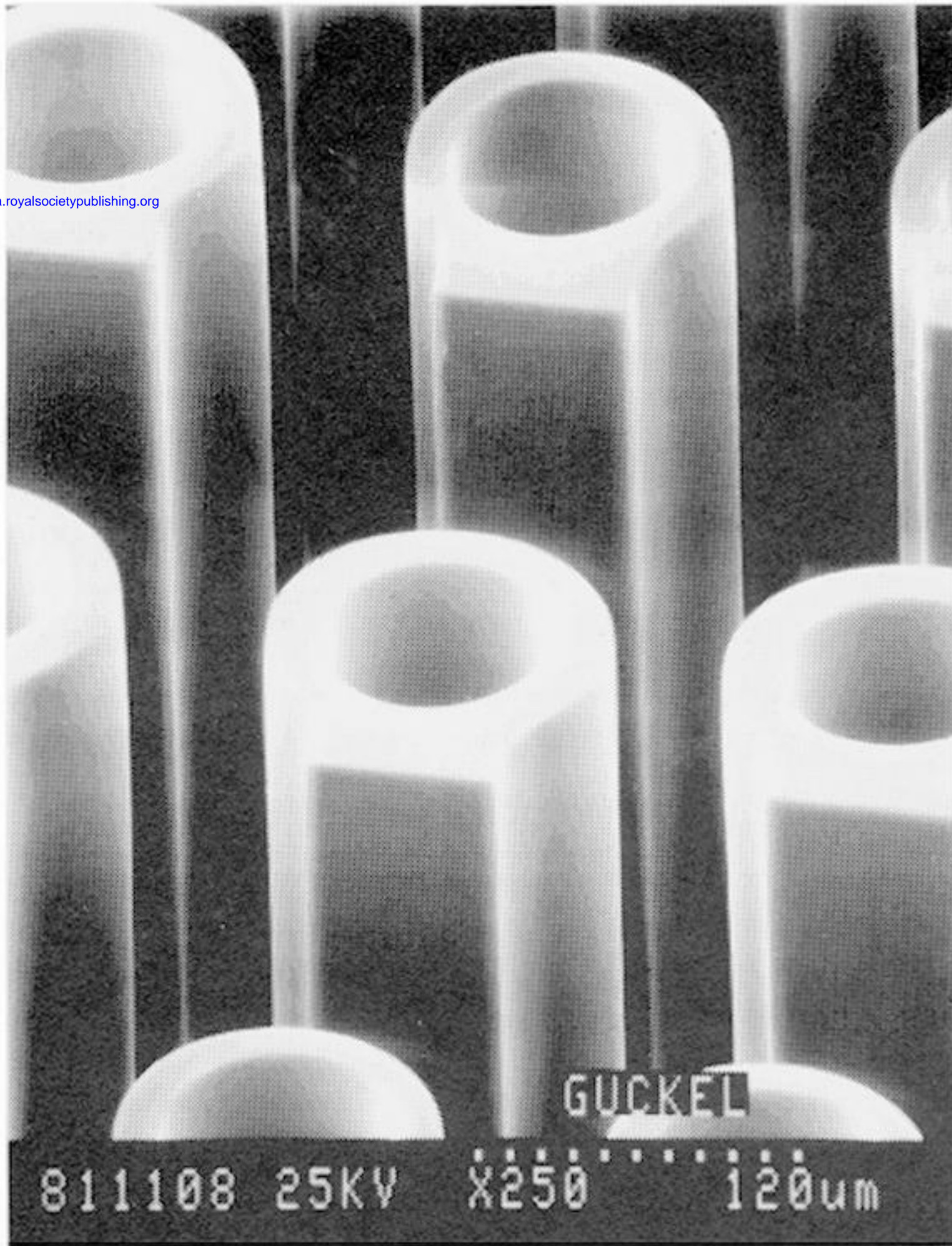
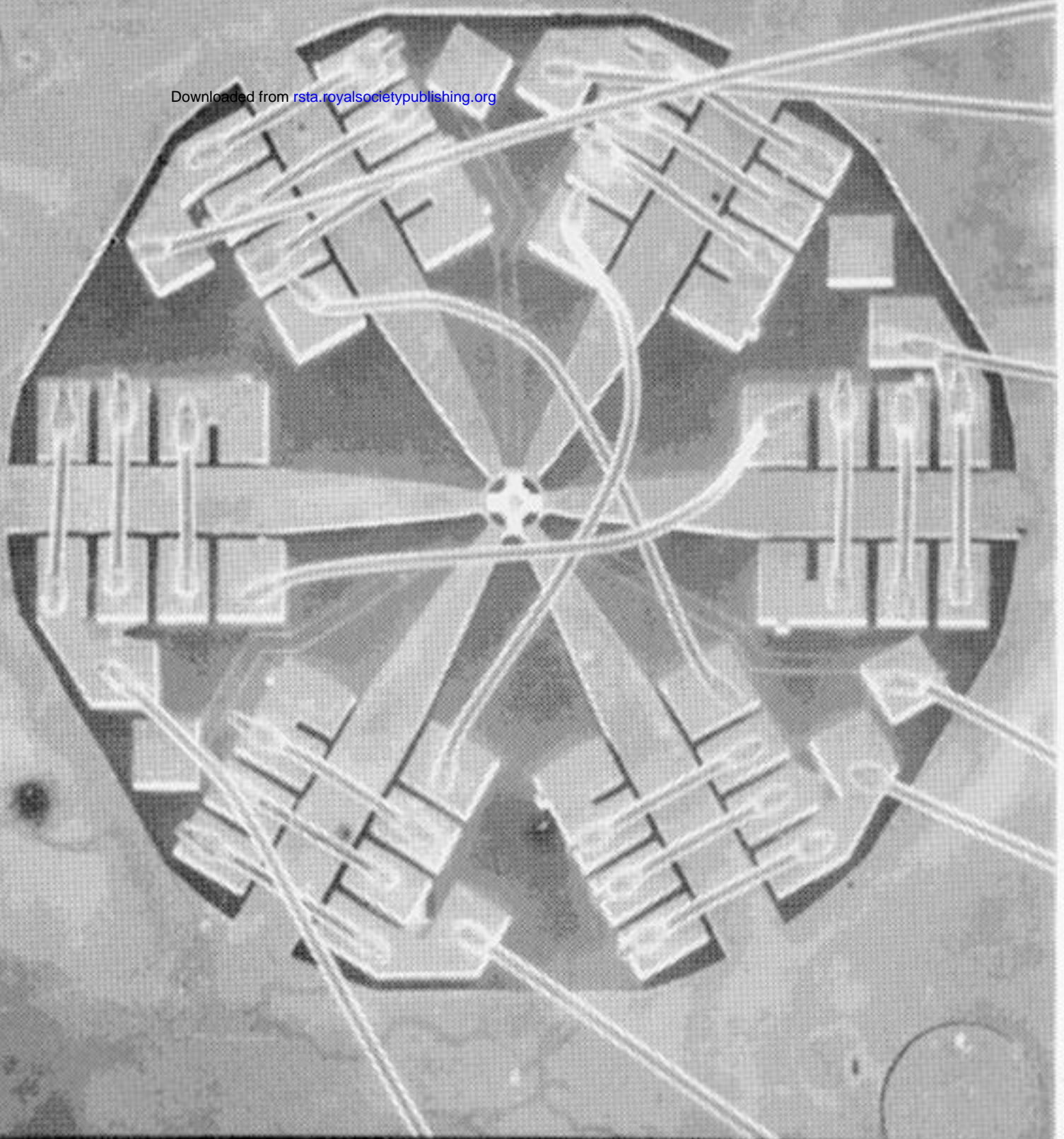


Figure 9. Exposed and developed PMMA pattern with structural height of 3200  $\mu\text{m}$ .



Downloaded from [rsta.royalsocietypublishing.org](http://rsta.royalsocietypublishing.org)



106007 10KV X35.0 .86mm

Figure 10. Three-phase micromotor.